Published in "Proceedings of the National Academy of Sciences
106 (25): 10314-10319, 2009" which should be cited to refer to this work.

Localized olfactory representation in mushroom bodies of *Drosophila* larvae

Liria M. Masuda-Nakagawa[a,1], Nanaë Gendre[b], Cahir J. O'Kane[c], and Reinhard F. Stocker[b]

[a]Institute of Molecular and Cellular Biosciences, University of Tokyo, Yayoi 1-1-1, Bunkyo-ku, Tokyo 113-0032, Japan; [b]Department of Biology, University of Fribourg, Chemin du Musée 10, CH-1700 Fribourg, Switzerland; and [c]Department of Genetics, University of Cambridge, Downing Street, Cambridge CB2 3EH, United Kingdom

Odor discrimination in higher brain centers is essential for behavioral responses to odors. One such center is the mushroom body (MB) of insects, which is required for odor discrimination learning. The calyx of the MB receives olfactory input from projection neurons (PNs) that are targets of olfactory sensory neurons (OSNs) in the antennal lobe (AL). In the calyx, olfactory information is transformed from broadly-tuned representations in PNs to sparse representations in MB neurons (Kenyon cells). However, the extent of stereotypy in olfactory representations in the calyx is unknown. Using the anatomically-simple larval olfactory system of *Drosophila* in which odor ligands for the entire set of 21 OSNs are known, we asked how odor identity is represented in the MB calyx. We first mapped the projections of all larval OSNs in the glomeruli of the AL, and then followed the connections of individual PNs from the AL to different calyx glomeruli. We thus established a comprehensive olfactory map from OSNs to a higher olfactory association center, at a single-cell level. Stimulation of single OSNs evoked strong neuronal activity in 1 to 3 calyx glomeruli, showing that broadening of the strongest PN responses is limited to a few calyx glomeruli. Stereotypic representation of single OSN input in calyx glomeruli provides a mechanism for MB neurons to detect and discriminate olfactory cues.

calyx | genetically-encoded calcium indicator | olfactory sensory neurons | projection neurons

We now understand much about how odor information is detected and conveyed to the brain by sensory neurons, but less about how this information is represented in higher brain centers to influence behavioral outputs. The mushroom body (MB) of insects, which in *Drosophila* is essential for odor discrimination learning, provides a model to understand olfactory coding in higher association centers (1, 2). In the periphery, odor identity is detected by sets of olfactory sensory neurons (OSNs) whose specificities are determined by the olfactory receptor (OR) that they express (3, 4). OSNs that express the same OR converge on defined glomeruli in the first olfactory center of the brain, the antennal lobe (AL), analogously to the convergence of OSNs on olfactory bulb glomeruli in mammals. Projection neurons (PNs) then carry olfactory information from single AL glomeruli to the higher brain, the MB, and the lateral horn. However, excitatory interneurons that innervate multiple AL glomeruli lead to broadening of PN specificity compared with OSNs (5, 6). PNs then connect to Kenyon cells (KCs) in the calyx of the MB, where the representation of odor qualities is radically transformed; individual KCs respond much more selectively to odors than do either OSNs or PNs (7–9).

The extent of stereotypy in olfactory processing in the calyx has been a matter of debate, in contrast to the clearly stereotypic connections between OSNs and PNs in the AL. In *Drosophila* adults, apparently stereotypic projections of PNs and KCs have been defined anatomically only at the level of broad zones (10–12), and odors can evoke localized PN activity in large regions of the calyx (13). However, at least some subsets of KCs show apparently nonstereotypic responses to odors (9). The level of spatial stereotypy of odor representations in PNs in the calyx has not yet been functionally defined, and the complexity of the adult calyx makes it difficult to visualize the representation of odor qualities in single identified cells.

Drosophila larvae, which can perceive a wide variety of odors (14) and perform odor discrimination learning (15, 16), have an olfactory system with the same basic architecture as adults but numerically much simpler. It contains only 21 unique OSNs (17), each expressing a different OR (3, 4) with known ligand specificity (18). Each AL glomerulus appears to be connected to the MB calyx by a single PN (19). Whereas the adult calyx consists of hundreds of microglomeruli that cannot be individually identified, the larval calyx is organized in ≈34 glomeruli, in each of which a single identifiable PN contacts hundreds of KC dendrites (20). Therefore, the larval olfactory system comprises a small number of identifiable odor quality channels, each carried by a single neuron between successive layers of the olfactory pathway.

Here, we use the simple larval calyx to ask how individual odor qualities are represented in PN terminals and individual calyx glomeruli. We first generated a 3D map of OSN projections in larval AL glomeruli. Using this map, we determined the connectivity of individual PNs between specific AL glomeruli and calyx glomeruli. Although the 1-to-1 connectivity between OSNs and PNs in AL glomeruli predicts that activity in each OSN should stimulate a single calyx glomerulus, it is not easy to predict how many calyx glomeruli are activated as a result of broadening of PN responses relative to OSNs. By carrying out the imaging of odor-evoked activity in single PN terminals in the intact larval MB, we detect only limited dispersal of olfactory signals during their transmission from single OSNs to the calyx.

Results

3D Map of the Larval AL Based on OSN Projections. To identify the main sensory pathways from OSNs into PNs in the larval AL, we first generated a 3D map of AL glomeruli, defined by the innervation patterns of larval OSNs. We analyzed confocal sections of the AL projections of 22 *OrX-GAL4* lines that are each expressed in a single OSN (3, 4). Terminals of single OSNs each ramified within a single AL glomerulus into branches and varicosities of variable number, density, size, and shape (Fig. 1*A*). The arrangement of OSN presynaptic terminals within glomeruli was confirmed by visualizing terminals of all OSNs using *n-syb*::*GFP* (Fig. 1*B*). In contrast, PN dendrites filled up most of the volume of AL glomeruli in which they arborized (Fig. 1*C*).

Author contributions: L.M.M.-N., C.J.O., and R.F.S. designed research; L.M.M.-N., N.G., and R.F.S. performed research; C.J.O. contributed new reagents/analytic tools; L.M.M.-N., N.G., C.J.O., and R.F.S. analyzed data; and L.M.M.-N., C.J.O., and R.F.S. wrote the paper.

The authors declare no conflict of interest.

[1]To whom correspondence should be addressed. E-mail: almasuda@mail.ecc.u-tokyo.ac.jp.

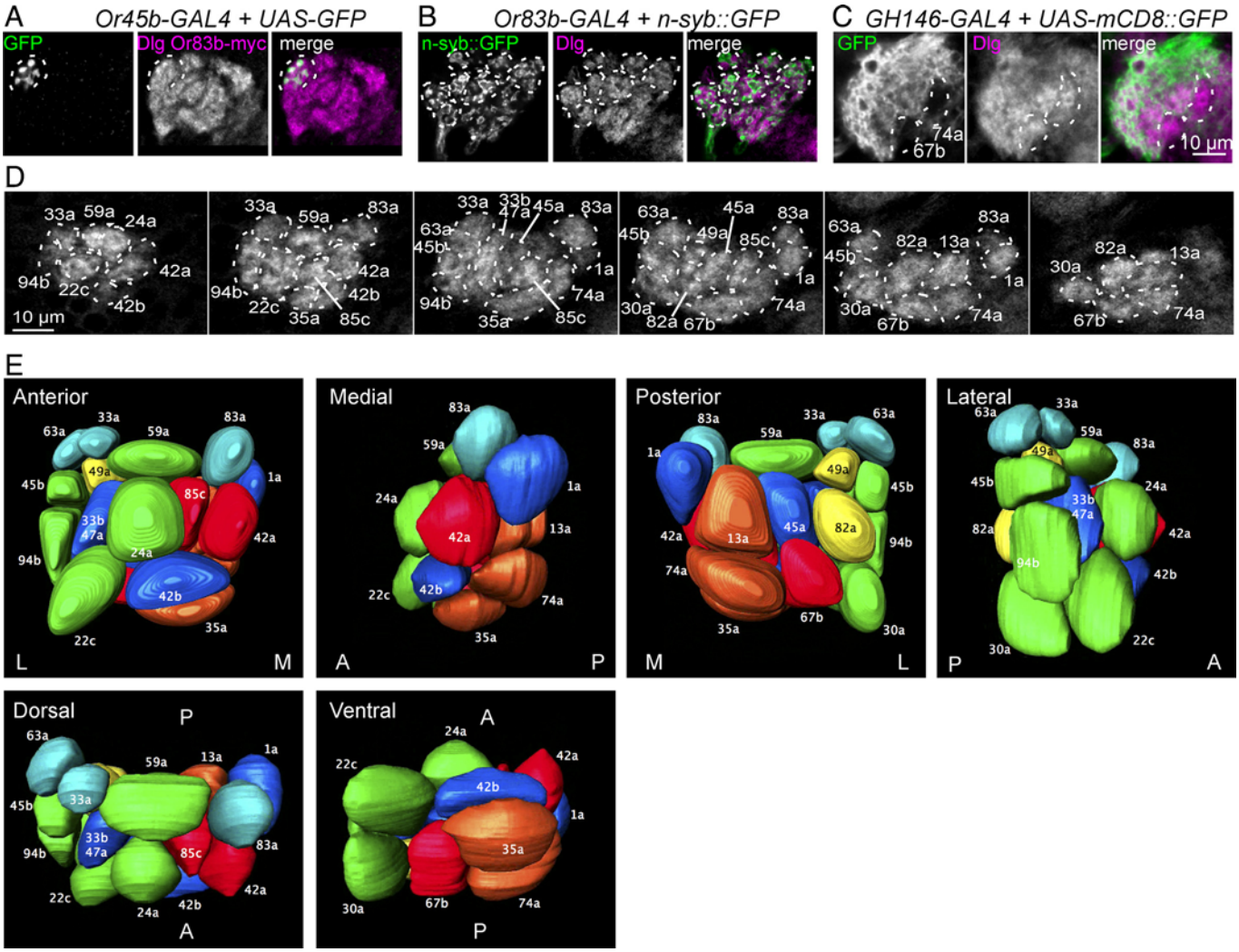

Fig. 1. 3D organization of the larval antennal lobe. All AL panels in this and subsequent figures show frontal confocal sections through the AL, with dorsal to the top, lateral to the left. (*A*) OSN terminals, labeled by expression of *GFP* under control of *Or45b-GAL4*, form varicosities within a single AL glomerulus (partly outlined by a broken line). (*B*) Expression of the synaptic vesicle marker *n-syb*::*GFP* in OSN presynaptic terminals using *Or83b-GAL4*, is found in varicosities within glomeruli (outlined by broken lines and labeled using anti-Dlg). (*C*) Arborization of *GH146* PN dendrites in a posterior section of a larval AL, in which *mCD8*::*GFP* is expressed using *GH146-GAL4*. Two glomeruli subsequently identified as 67b and 74a (broken lines) are not labeled by *GH146*. (*D*) Confocal sections from successive anteroposterior (AP) levels (from left to right, increments of 4 μm) of a representative larval AL, stained by anti-Dlg. Although glomeruli are not always completely separated from each other, prominent glomeruli are distinct (broken lines). For a complete AP sequence and for panels free of annotations, see Fig. S4. (*E*) 3D model of the larval AL, viewed from different angles. A, P, M, and L denote anterior, posterior, medial, and lateral faces of the AL, respectively. Full rotations of the model are in Movie S2 and Movie S3. Colors of glomeruli denote predicted responses to broad classes of odorant (18): green, aromatic; red, broad-range aliphatic, principally esters and ketones; blue, esters; brown, alcohols; yellow, inhibitory responses; pale blue, no known responses.

In general, glomerular position, shape and size were conserved between individuals (Fig. S1). The average center positions of 21 glomeruli were mapped by calculating the relative positions of OSN terminals within a virtual grid constructed from the average dimensions of the larval AL (Figs. S1–S3 and Table S1). Most of the glomeruli could be identified by anti-Dlg neuropile labeling that showed them as discrete structures at conserved locations, even though the borders were not always clearly defined (Fig. 1*D* Fig. S4, and Movie S1). Based on the typical terminal positions of each OSN, and visualization of glomerular outlines using anti-Dlg, we prepared a 3D glomerular model that allows inspection of the larval AL from different angles (Fig. 1*E*, Movies S2 and S3) and as a series of sections along the antero-posterior axis (Fig. S4).

Arborization of PN Dendrites in Single AL Glomeruli. We next tested whether PN dendritic arbors could be mapped onto specific AL glomeruli. Labeled PN clones were generated by FLP-out (21) in the *GH146-GAL4* line (Fig. 2*A*), reported to label ≈16–18 larval PNs (22). *GH146*-expressing PNs arborized throughout most AL glomeruli except for 67b and 74a (Fig. 1*C*), suggesting that the arborizations of PNs in 19 glomeruli could be studied by this approach. Arborizations of 142 labeled PNs in the AL clearly matched the glomerular organization of OSN terminals, thus allowing the identification of 19 classes of PN according to their overlap with the terminals of specific OSNs (examples in Fig. S5). PN arborizations were distributed more uniformly within glomeruli, covered a larger volume than OSN terminals, and sometimes sent collateral dendrites into neighboring glomeruli (Fig. S5).

Representation of OSN Input by PNs in the MB Calyx. To understand how the sensory map of the larval AL is represented in calyx glomeruli, we used the *GH146* PN clones described above. We identified calyx glomeruli by using published criteria of their

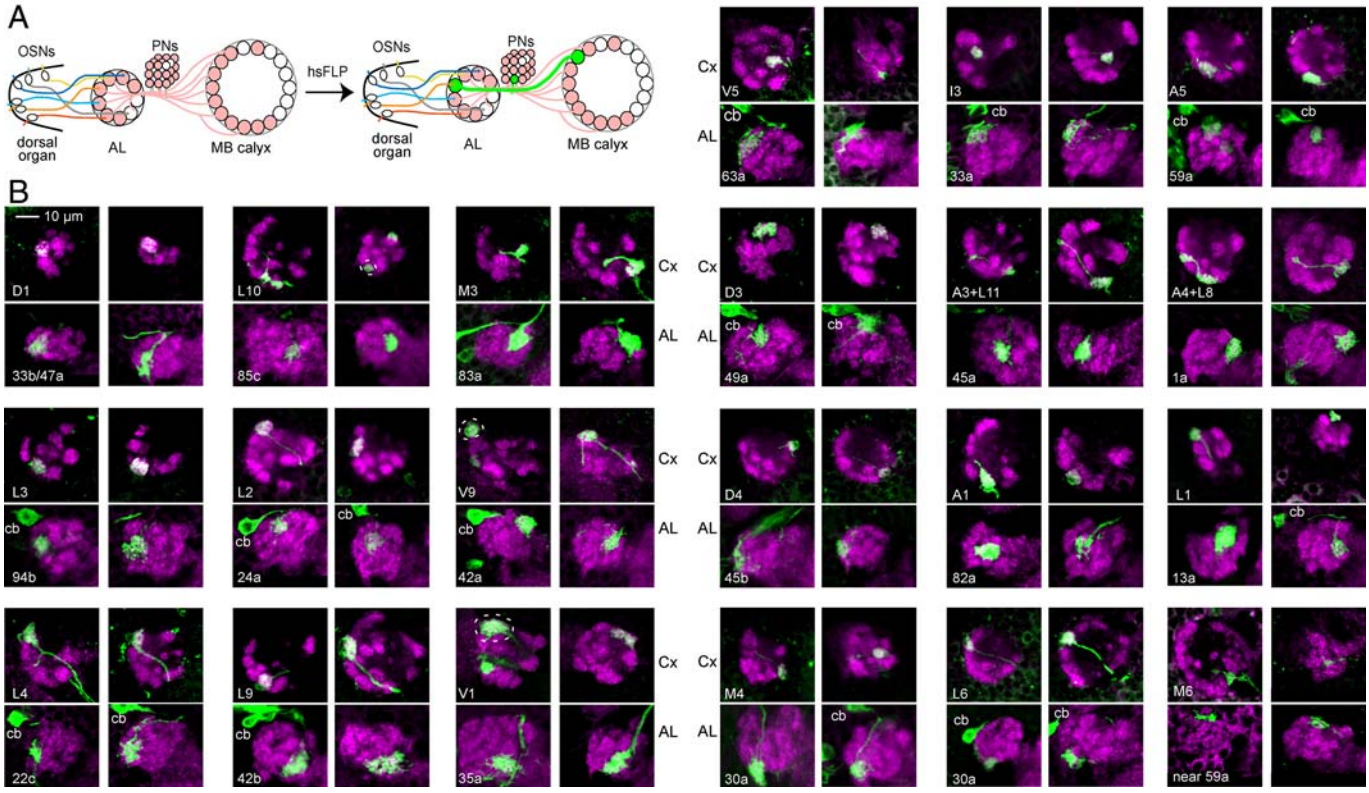

Fig. 2. Consistent connectivity by PNs between specific AL glomeruli and calyx glomeruli. (*A*) Generation of FLP-out clones in GH146-GAL4-expressing cells (shaded) by hsFLP expression labels different single PNs (example in green) including their projections in both AL and calyx. (*B*) Each pair of panels shows the same PN, labeled with *mCD8::GFP* (green), with presynaptic terminals in the calyx (Cx, upper panel of each pair) and dendritic arborizations in the AL (lower panel of each pair). Two preparations (left pair and right pair) are shown for each class of PN. Shown are projections of confocal sections, with total thicknesses between 3 and 10 μm. Calyx sections here and subsequently are viewed from a posterodorsal angle (Fig. S2), with anterior to the bottom and lateral to the left. In preparations with 2 labeled PNs, the designated glomeruli are highlighted by broken lines. cb, cell body.

positions relative to KC axon tracts and a few prominent calyx glomeruli at recognizable positions (20), and a new criterion, the AL glomerulus in which each of the 19 classes of PN arborized (see above). For the vast majority of PNs, we found consistent patterns of connectivity between specific AL glomeruli and specific calyx glomeruli (Fig. 2*B*; Tables S2 and S3). In total we analyzed 70 single-PN clones and an additional 84 neurons from 2-PN clones. In the latter cases we could not follow the trajectories of single PNs from the AL to the calyx. However, the AL and calyx glomeruli labeled in 2-cell clones were almost invariably consistent with them being combinations of the AL–calyx pairs labeled in single PN clones. Therefore, we used the 2-cell clones as supporting data for the matches found by using single-PN clones. Our conclusions are based on an average of 7 labeled PNs per AL glomerulus. From the 154 analyzed PNs, 148 showed a consistent pattern of connectivity between identified AL and identified calyx glomeruli (Table S3).

In total, we identified 23 calyx glomeruli receiving input by PNs from the 19 AL glomeruli, which matches the previous estimate of 23 *GH146*-positive calyx glomeruli (20). Although the general positions of calyx glomeruli connected to the same AL glomerulus were conserved, they appeared more variable than AL glomeruli (Fig. 2*B*). However, we reproducibly identified most (17/23) of the previously-designated (20) *GH146*-positive calyx glomeruli (Table S2 and Fig. 3). We also revised the designations of 6 calyx glomeruli to better reflect their positions in light of our ability to identify the PNs innervating them (Table S2).

Sixteen AL glomeruli were stereotypically connected with a single calyx glomerulus at consistent locations. Two other PNs (1a and 45a) connected a single AL glomerulus to 1 or a few calyx glomeruli (Tables S2 and S3). Finally, different PNs that appeared to arborize in AL glomerulus 30a innervated 2 different calyx glomeruli: either a ventromedial calyx glomerulus that we designated M4 (5 preparations) or a lateral calyx glomerulus that we termed L6 (5 preparations).

We found 2 additional classes of *GH146*-positive cell that innervated the calyx. First, a PN with its cell body far posterior ventrolateral to the AL arborized close to AL glomerulus 59a; its axon joined the tract connecting the AL with the calyx more posteriorly than other PNs and innervated calyx glomerulus M6 (Fig. 2*B*) and the lateral horn. Second, calyx glomerulus V3 was innervated by a neuron that is not an olfactory PN, but appeared to be a previously-described cell (23) with a dendritic field in the suboesophageal ganglion (Fig. S6 and Movie S4).

Activity Evoked by Single OSN Input in the MB Calyx. Because AL glomeruli are each innervated by the terminals of a single OSN, and predominantly by the dendrites of a single PN that usually innervates a single calyx glomerulus, a simple expectation is that activity in each OSN should evoke activity mostly in a single calyx glomerulus. We therefore tested the representation of 3 single OSNs in the calyx, by recording the pattern of activity in calyces of larvae that had only a single functional OSN (3) and expressed *GCaMP1.3* in PNs (Fig. 4*A*).

As predicted, odor stimulation of OSN 42a consistently activated a single calyx glomerulus, usually in the ventral posterolateral part of the calyx (Fig. 4*B*). This location is in agreement with the innervation of calyx glomerulus V9 by PNs whose dendrites innervate AL glomerulus 42a (Figs. 2*B* and 3). We

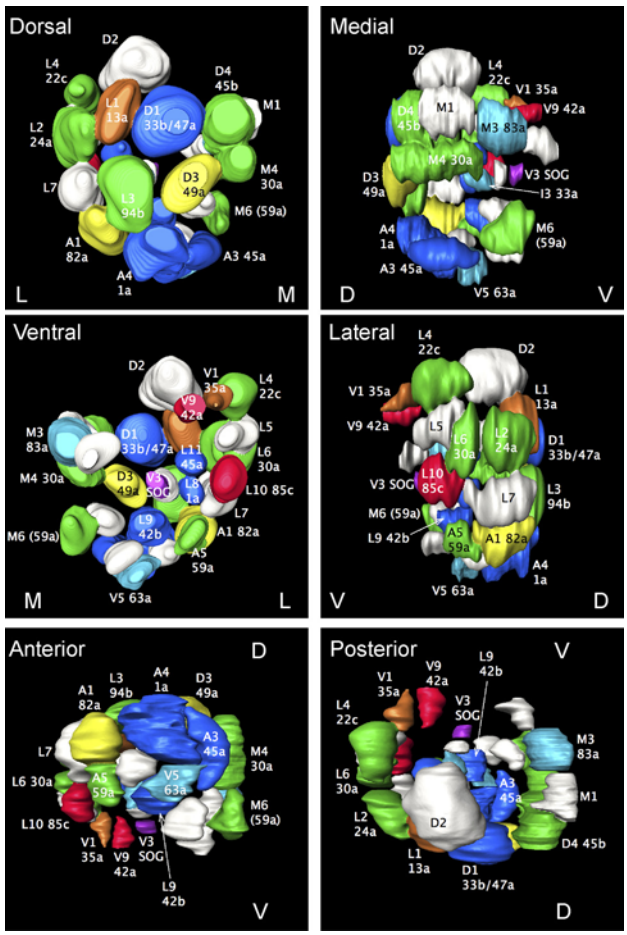

Fig. 3. OSN representation in calyx glomeruli. This is a 3D reconstruction of a single calyx, viewed from different angles. *GH146*-expressing glomeruli are color-coded according to predicted input as in Fig. 1*E*; other glomeruli are white. Labeling indicates both the name of the best-fitting calyx glomerulus and the AL glomerulus connected to it. D, V, M, and L denote dorsal, ventral, medial, and lateral faces of the calyx, respectively.

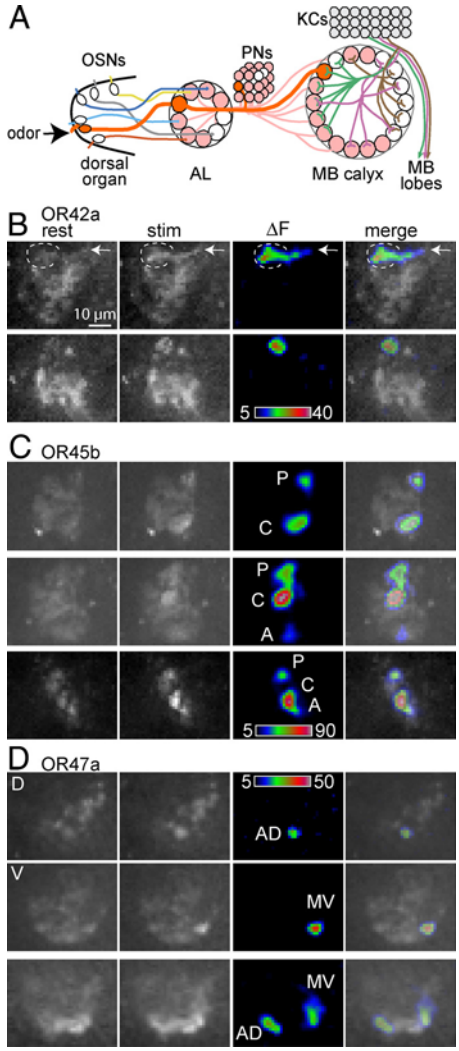

Fig. 4. PN activity in the calyx of larvae with a single functional OSN. (*A*) Diagram of the larval olfactory circuitry, showing GCaMP1.3 expressed in most PNs under control of GH146-GAL4 (shaded PNs that project to AL and calyx). A single functional OSN is expected to strongly stimulate a single PN that normally has a presynaptic terminal in a single calyx glomerulus (pathway shown by dark thick shading). (*B–D*) Each row shows GCaMP fluorescence in *GH146*-expressing PN terminals of a single calyx at rest and during stimulation, with ΔF represented in false color, both alone and superimposed on a raw image. Panels are single confocal sections, except where noted. Quantification and time courses of responses are shown in Fig. S7. (*B*) Activity in ventral sections of 2 calyces, evoked by ethyl acetate via OSN 42a. Note the increased fluorescence in 1 calyx glomerulus, possibly V9. In the top row the active glomerulus is surrounded by a broken line, and activity is also seen in an axon coming from the inner antennocerebral tract (arrow). (*C*) Activity in 3 calyces, evoked by acetophenone via OSN 45b. The top and middle rows come from different brain hemispheres of the same larva (all calyces are presented with lateral left and anterior front, for consistency between panels). Most calyces show a strongly-responding posterior (P) glomerulus, possibly D4, and a central (C) glomerulus, and a few have a more weakly responding anterior (A) glomerulus. The middle row shows 2 superimposed sections from midway (P glomerulus) and ventral (C and A glomeruli) levels along the dorsoventral axis. (*D*) Activity in 2 calyces, evoked by pentyl acetate via OSN 47a. The first 2 rows show dorsal (D) and ventral (V) sections from the same calyx. Most glomeruli show activity in an anterodorsal (AD) glomerulus, possibly D1, and a medioventral (MV) glomerulus.

were unable to map the active glomerulus more accurately in live preparations, because brain orientation was more variable than in fixed preparations and Dlg background staining could not be applied.

Unexpectedly, odor stimulation of either OSN 45b or 47a usually activated 2 calyx glomeruli strongly (Fig. 4 *C* and *D*). Approximately a quarter of preparations also had a third glomerulus that showed weak activity (e.g., Fig. 4*C*), and occasional brains had only a single active glomerulus. For both OSNs, 1 active glomerulus was usually in a location expected from the PN clonal analysis: in the case of OSN 45b, one was in the posteromedial region of the calyx, consistent with the expectation of activity in glomerulus D4, and in the case of OSN 47a, an anterodorsal glomerulus consistent with the expectation of activity in glomerulus D1 (Figs. 2*B* and 3) was found. The other active glomeruli tended to be found in an anterior or central location in the case of OSN 45b stimulation and in a ventromedial location in the case of OSN 47a, but because of the absence of landmarks in the live preparations we were not able to assign their identities.

Discussion

Parallel Pathways from OSNs to the Calyx. We have generated a comprehensive olfactory circuit analysis that links identified sensory neurons to localized activity in a higher association center and shows how activity in identified sensory neurons is represented in such a center.

We provide a 3D larval AL glomerular map of the input of the whole set of 21 OSN classes. Comparison of the map with the

ligand specificities of larval ORs (18) shows a regional representation of some classes of odor qualities. For example, aromatic odors are represented mainly in a cluster of lateral glomeruli, whereas alcohols appear to map to medial glomeruli (Fig. 1*E*; Movie S2, and Movie S3). The proximity of AL glomeruli dealing with similar odor qualities may facilitate cross-talk by local interneurons between glomeruli, broadening olfactory representations during their passage through the AL, but preferentially among subsets of PNs that deal with similar odor qualities.

The criterion of AL glomerular arborization to identify PNs supports most features of the previous calyx map (20) and refines it by providing a potential molecular criterion for identifying calyx glomeruli. We thus identified 23 calyx glomeruli that receive input from 19 AL glomeruli. In almost all cases, each AL glomerulus and OSN is represented uniquely by 1 or 2 calyx glomeruli. Unexpectedly, 1 apparent PN class (30a), innervates calyx glomeruli at 2 alternative positions (L6 and M4), and specific PN molecular markers will probably be required to determine whether this is really a single class of PN.

In the calyx, the representation of odor quality classes appears more dispersed than in the AL. For example, "aromatic" AL glomeruli are connected to calyx glomeruli that are not obviously clustered. Also, the neighboring AL glomeruli 13a and 35a, which respond preferentially to alcohols, innervate nonadjacent calyx glomeruli L1 and V1. Similar patterns are seen for the calyx representations of other functionally-related groups of AL glomeruli (Figs. 2*B* and 3, Movie S5, and Movie S6). Because most KCs can integrate inputs from widely dispersed and apparently random subsets of calyx glomeruli (20), spatial proximity of glomeruli may be less important for processing olfactory representations in the calyx than in the AL, where the spatial organization of OSN input and PN output is very stereotypic.

GH146-positive PNs innervate only 22 of some 34 calyx glomeruli. From where do the remaining calyx glomeruli receive their input? Candidates are non-*GH146*-expressing PNs innervating AL glomeruli 67b and 74a or nonolfactory neurons such as the one providing input to V3 from a broad region of the suboesophageal ganglion, the main gustatory input region in the larva (23). Neurons transmitting gustatory signals into the calyx could allow larvae to use taste and smell as conditioned stimuli in associative learning.

Evoked Activity in Calyx Glomeruli. Our single-clone analysis suggests that each PN essentially connects a single AL glomerulus to a single calyx glomerulus. Consistent with this, stimulation of OSN 42a activated a single calyx glomerulus, whose position was consistent with it being V9, which is connected to AL glomerulus 42a.

In contrast, stimulation of either OSN 45b or OSN 47a strongly activated 2 calyx glomeruli in most preparations, with weak activation of an additional calyx glomerulus in a few preparations. For both OSNs, the position of 1 activated glomerulus was generally consistent with the predictions from the PN clonal analysis, but the presence of additional active glomeruli was unexpected. While our work was under review, Asahina et al. (24) also reported that stimulation of single OSNs activated PN terminals strongly in either 1 or 2 calyx glomeruli and suggested that this finding was consistent with a 1-to-1 connectivity between OSNs and PNs in the AL.

Although our observations of strong activity evoked by single OSNs in 1 to 3 calyx glomeruli are remarkably consistent with Asahina et al. (24), our analysis of the neuronal circuitry leads us to a very different interpretation. OSNs 45b and 47a (this work) and 42b (24) all evoke activity in multiple calyx glomeruli, but the PNs that connect to these OSNs in the AL innervate only a single calyx glomerulus; activity in multiple calyx glomeruli therefore cannot be explained by a 1-to-1 connectivity between OSNs and PNs. At least 2 explanations are possible. First, AL glomeruli 45b and 47a might each contain arborizations from 2 PNs, each of which innervates a different calyx glomerulus. However, this is unlikely, because arborizations of >1 *GH146*-positive PN in a single larval AL glomerulus were never observed (19). Second, interglomerular excitatory cholinergic connections in the AL, which apparently follow defined routes, broaden the response of PNs relative to that of OSNs (5, 6, 25). Olsen et al. (5) detected broadening of input from single adult OSNs to many more PNs than the one or two observed here, in the form of depolarization of most PNs tested, from a subset of the entire PN population. However, they reported only occasional spikes. In contrast, our imaging experiments assay almost all PNs for presynaptic activity, and we detect probably high levels of spiking in one or a few PN terminals, because GCaMP may not be sensitive enough to detect lower levels of activity (26). Either the larval and adult calyces differ in the nature of lateral excitatory spread, or the limited set of OSN and PN combinations sampled by Olsen et al. (5) may have missed high levels of lateral excitation of a small number of PNs. In conclusion, the high levels of activity in a small number of larval calyx glomeruli are consistent with specific routes for broadening of some olfactory representations in the AL, but suggest that the strongest signals from single OSNs are not widely dispersed in the calyx.

Conclusions

The simple organization of the *Drosophila* larval olfactory system has facilitated both a 3D sensory map of the larval AL of *Drosophila* and a map of the major OSN input to specific glomeruli in the calyx. Together with the apparently random arborization of KC dendrites among calyx glomeruli, this work suggests that KCs may receive many different combinations of heterogeneous odor inputs, allowing them to discriminate very large numbers of odor bouquets. The future availability of GAL4 lines that permit activation or silencing of spatially-localized inputs into the calyx, or the ability to visualize activity of specific input pathways, should help to reveal how representations of odor qualities are transformed in the calyx and how they are encoded by KCs during learning.

We have produced a map of sensory input to a defined association center in the higher brain. The most analogous (and possibly homologous) regions in the vertebrate brain are association cortices, including olfactory cortex areas, where no overt spatial organization of sensory inputs has been detected. The larval calyx provides a very clear picture of how sensory inputs are organized and can potentially be a model for more complex association centers where the complexity obscures the underlying logic of the connectivity.

Materials and Methods

Fly Strains and Clone Induction. Flies were raised on standard cornmeal medium at 25 °C. OSNs were labeled by crossing *Or83b-Myc*;*UAS-GFP* (3) to *OrX-GAL4* lines (4). *UAS-nsyb*::*GFP* has been described by Ito et al. (27). PN clones were generated by FLP-out, in the progeny of, *GH146-GAL4* (28, 29) crossed to *hsFLP*;*CyO/Sp*;*UAS*> y^+ *CD2*>*CD8-GFP* (21). FLP recombinase was induced by heat shock (35 °C) for 20–30 min at 12–18, 18–24, or 24–30 h after egg laying. Neuronal activity in PN terminals of larvae with a single active OSN was imaged in the female progeny of *GC56*;*GH146-GAL4/CyO*;*or83b*^{1} females crossed to *GC56/Y*;*OrX-GAL4*;*or83b*^{1} males. *GC56* is an X chromosome with 2 copies of *UAS-GCaMP1.3* (30). *OrX-GAL4* insertions (Fig. S8) were either homozygous *Or42a-GAL4* or *Or47a-GAL4*, or *Or45b-GAL4* heterozygous with *CyO*.

Specimen Orientation and Confocal Immunomicroscopy. The CNS of wandering third-instar larvae was dissected, fixed, and labeled as described (20). Orientation of the larval AL was defined relative to the body axis rather than the neuraxis, as described in *SI Text* and Fig. S2. To collect confocal images from the larval MB calyx, the CNS was viewed from a posterodorsal angle as described (20) (Fig. S2). This allowed more standardized orientation of calyx landmarks than the flattened preparation of Ramaekers et al. (19) and easier comparison

with imaging of calyx activity; we therefore adopted the nomenclature of Masuda-Nakagawa et al. (20) for calyx glomeruli.

Imaging Neuronal Activity in Calyx. Females were identified by the lack of testis at the wandering stage and dissected in HL3 medium containing 1.5 mM Ca^{2+} (31) to expose their brain. The dorsal organ was exposed to air, pointing down through a hole in a paraffin membrane that rested on 2 silicone spacers on a glass slide. The brain above this was bathed in HL3, beneath a coverslip that rested lightly on the larva and paraffin membrane. Larvae were exposed to a stream of air that could be switched to a stream of air that contained odorant, as described in *SI Text*. GCaMP fluorescence was visualized with a spinning disc confocal microscope and analyzed as described in *SI Text*.

ACKNOWLEDGMENTS. We thank L. Vosshall (Rockefeller University, New York), J. Carlson (Yale University, New Haven, CT), and B. Dickson (Institute for Molecular Pathology, Vienna) for *OrX-GAL4* lines; R. Axel (Columbia University, New York) for *UAS-GCaMP1.3*; the Developmental Studies Hybridoma Bank (University of Iowa, Iowa City) for anti-Dlg and 9E10; the Yokogawa Corporation (Tokyo) for the loan of spinning disc scanner CSU-22; K. Ito for generous provision of microscopy facilities and lab space (to L.M.M.-N.); and M. Tanifuji and S. Namiki for advice on odor delivery. This work was supported by Japan Society for the Promotion of Science Grant-in-Aid for Scientific Research 19500265 (to L.M.M.-N.), U.K. Biotechnology and Biological Sciences Research Council Grant BBS/B/06954 (to C.J.O.), and Swiss National Funds Grants 31-63447.00 and 3100A0-105517 (to R.F.S.).

1. Heisenberg M (2003) Mushroom body memoir: From maps to models. *Nat Rev Neurosci* 4:266–275.
2. Davis RL (2005) Olfactory memory formation in *Drosophila*: From molecular to systems neuroscience. *Annu Rev Neurosci* 28:275–302.
3. Fishilevich E, et al. (2005) Chemotaxis behavior mediated by single larval olfactory neurons in *Drosophila. Curr Biol* 15:2086–2096.
4. Kreher SA, Kwon JY, Carlson JR (2005) The molecular basis of odor coding in the *Drosophila* larva. *Neuron* 46:445–456.
5. Olsen SR, Bhandawat V, Wilson RI (2007) Excitatory interactions between olfactory processing channels in the *Drosophila* antennal lobe. *Neuron* 54:89–103.
6. Shang Y, Claridge-Chang A, Sjulson L, Pypaert M, Miesenböck G (2007) Excitatory local circuits and their implications for olfactory processing in the fly antennal lobe. *Cell* 128:601–612.
7. Perez-Orive J, et al. (2002) Oscillations and sparsening of odor representations in the mushroom body. *Science* 297:359–365.
8. Stopfer M, Jayaraman V, Laurent G (2003) Intensity versus identity coding in an olfactory system. *Neuron* 39:991–1004.
9. Murthy M, Fiete I, Laurent G (2008) Testing odor response stereotypy in the *Drosophila* mushroom body. *Neuron* 59:1009–1023.
10. Tanaka NK, Awasaki T, Shimada T, Ito K (2004) Integration of chemosensory pathways in the *Drosophila* second-order olfactory centers. *Curr Biol* 14:449–457.
11. Jefferis GSXE, et al. (2007) Comprehensive maps of *Drosophila* higher olfactory centers: Spatially segregated fruit and pheromone representation. *Cell* 128:1187–1203.
12. Lin H-H, Lai JS-Y, Chin A-L, Chen Y-C, Chiang A-S (2007) A map of olfactory representation in the *Drosophila* mushroom body. *Cell* 128:1205–1217.
13. Fiala A, et al. (2002) Genetically encoded cameleon in *Drosophila melanogaster* is used to visualize olfactory information in projection neurons. *Curr Biol* 12:1877–1884.
14. Cobb M (1999) What and how do maggots smell? *Biol Rev* 74:425–459.
15. Aceves-Piña EO, Quinn WG (1979) Learning in normal and mutant *Drosophila* larvae. *Science* 206:93–96.
16. Scherer S, Stocker RF, Gerber B (2003) Olfactory learning in individually assayed *Drosophila* larvae. *Learn Mem* 10:217–225.
17. Singh RN, Singh K (1984) Fine structure of the sensory organs of *Drosophila melanogaster* Meigen larva (Diptera: Drosophilidae). *Int J Insect Morphol Embryol* 13:255–273.
18. Kreher SA, Mathew D, Kim J, Carlson JR (2008) Translation of sensory input into behavioral output via an olfactory system. *Neuron* 59:110–124.
19. Ramaekers A, et al. (2005) Glomerular maps without cellular redundancy at successive levels of the *Drosophila* larval olfactory circuit. *Curr Biol* 15:982–992.
20. Masuda-Nakagawa LM, Tanaka NK, O'Kane CJ (2005) Stereotypic and random patterns of connectivity in the larval mushroom body calyx of *Drosophila. Proc Natl Acad Sci USA* 102:19027–19032.
21. Wong AM, Wang JW, Axel R (2002) Spatial representation of the glomerular map in the *Drosophila* protocerebrum. *Cell* 109:229–241.
22. Marin EC, Watts RJ, Tanaka NK, Ito K, Luo L (2005) Developmentally programmed remodeling of the *Drosophila* olfactory circuit. *Development* 132:725–737.
23. Colomb J, Grillenzoni N, Ramaekers A, Stocker RF (2007) Architecture of the primary taste center of *Drosophila melanogaster* larvae. *J Comp Neurol* 502:834–847.
24. Asahina, K, Louis M, Piccinotti S, Vosshall LB (2009) A circuit supporting concentration-invariant odor perception in *Drosophila. J Biol* 8:9.
25. Bhandawat V, Olsen SR, Gouwens NW, Schlief ML, Wilson RI (2007) Sensory processing in the *Drosophila* antennal lobe increases reliability and separability of ensemble odor representations. *Nat Neurosci* 10:1474–1482.
26. Jayaraman V, Laurent G (2007) Evaluating a genetically encoded optical sensor of neural activity using electrophysiology in intact adult fruit flies. *Front Neur Circuits* 1:3.
27. Ito K, et al. (1998) The organization of extrinsic neurons and their implications in the functional roles of the mushroom bodies in *Drosophila melanogaster* Meigen. *Learn Mem* 5:52–77.
28. Stocker RF, Heimbeck G, Gendre N, de Belle JS (1997) Neuroblast ablation in *Drosophila* P[GAL4] lines reveals origins of olfactory interneurons. *J Neurobiol* 32:443–456.
29. Heimbeck G, Bugnon V, Gendre N, Keller A, Stocker RF (2001) A central neural circuit for experience-independent olfactory and courtship behavior in *Drosophila melanogaster. Proc Natl Acad Sci USA* 98:15336–15341.
30. Wang JW, Wong AM, Flores J, Vosshall LB, Axel R (2003) Two-photon calcium imaging reveals an odor-evoked map of activity in the fly brain. *Cell* 112:271–282.
31. Stewart BA, Atwood HL, Renger JJ, Wang J, Wu C-F (1994) Improved stability of *Drosophila* neuromuscular junction preparations in haemolymph-like physiological solutions. *J Comp Physiol A* 175:179–191.